Nonergodic one-magnon magnetization dynamics of the antiferromagnetic delta chain

Florian Johannesmann, Jannis Eckseler, Henrik Schlüter, and Jürgen Schnack*
Fakultät für Physik, Universität Bielefeld, Postfach 100131, D-33501 Bielefeld, Germany

(Received 21 March 2023; revised 17 July 2023; accepted 24 July 2023; published 4 August 2023)

We investigate the one-magnon dynamics of the antiferromagnetic delta chain as a paradigmatic example of tunable equilibration. Depending on the ratio of nearest and next-nearest exchange interactions the spin system exhibits a flat band in one-magnon space—in this case equilibration happens only partially, whereas it appears to be complete with dispersive bands as generally expected for generic Hamiltonians. We provide analytical as well as numerical insight into the phenomenon.

DOI: 10.1103/PhysRevB.108.064304

I. INTRODUCTION

Recent theoretical investigations on the foundations of thermodynamics focus on equilibration as well as thermalization in closed quantum systems under unitary time evolution. The road to a deeper understanding was paved by the seminal papers of Deutsch, Srednicki, and many others [1–12]. In simple words, the accepted expectation is that generic Hamiltonians, i.e., Hamiltonians that are not special but rather represent a class of similar Hamiltonians, lead to equilibration for the vast majority of initial states [13]. In this context it appears interesting to understand the *untypical* behavior seen for *special* Hamiltonians or special states such as quantum scar states [14–19].

For numerical studies, spin systems are the models of choice both since they are numerically feasible due to the finite size of their Hilbert spaces as well as they are experimentally accessible for instance in standard investigations by means of electron parametric resonance (EPR), free induction decay (FID), or in atomic traps (see, e.g., Refs. [20–25]). In such systems, observables assume expectation values that are practically indistinguishable from the prediction of the diagonal ensemble for the vast majority of all late times of their time evolution under very general and rather not restrictive conditions (see, e.g., Refs. [7,26–32]).

In the present paper we investigate the paradigmatic spin delta chain in the Heisenberg model which becomes special for a certain ratio of the two defining exchange interactions J_1 and J_2 (see Fig. 1). For $J_2/J_1 = 1/2$ the system exhibits a flat band in one-magnon space or equivalently independent localized one-magnon eigenstates of the Hamiltonian, a phenomenon that has been attracting great attention for more than 20 years now (see, e.g., Refs. [33–45]). In the context of equilibration, flat bands are interesting since they give rise to zero group velocity and thus result in a special form of (partial) localization, sometimes also termed disorder-free localization [17].

Since the one-magnon space of the delta chain hosts only two energy bands (two spins per unit cell) the quantum problem can be solved analytically. We will present both analytical as well as numerical solutions of the time-dependent Schrödinger equation and in particular investigate the magnetization dynamics with and without a flat band. We will provide analytical insight into which parts of an initial state will not participate in the process of equilibration. Our results can be qualitatively transferred to other flat-band systems such as kagome, square kagome, or pyrochlore spin systems.

The paper is organized as follows. In Sec. II we introduce the model, the concept of independent localized magnons, as well as the major results. Section III provides the technical details. The paper closes with a discussion in Sec. IV.

II. ONE-MAGNON DYNAMICS OF THE DELTA CHAIN

The antiferromagnetic delta chain is displayed in Fig. 1 (top). It is modeled by the Heisenberg model where the spin sites are enumerated as $0, 1, \ldots, N-1$ and the Nth site is equivalent to the zeroth site, $N \equiv 0$, assuming periodic boundary conditions

$$\underset{\sim}{H} = -2J_1 \sum_{i=0}^{N-1} \underset{\sim}{\vec{s}}_i \cdot \underset{\sim}{\vec{s}}_{i+1} - 2J_2 \sum_{i=0}^{\frac{N}{2}-1} \underset{\sim}{\vec{s}}_{2i} \cdot \underset{\sim}{\vec{s}}_{2i+2}, \tag{1}$$

where $\underset{\sim}{\vec{s}}_i$ denote spin vector operators and $J_1 < 0$ as well as $J_2 < 0$ are antiferromagnetic exchange interactions. The model can be treated analytically in one-magnon space, i.e., when the total magnetic quantum number is given by $M = N(s_a + s_b)/2 - 1$. Since the chain hosts two spins per unit cell the eigenenergies are split into two bands of which one is flat for $\alpha = J_2/J_1 = 1/2$ [compare Fig. 1 (bottom)]. In the latter case, one can transform the states of the flat band into independent localized one-magnon states [see Fig. 1 (top) and, e.g., Refs. [34,42]],

$$\begin{aligned} |\phi_\mu^0\rangle &= \frac{1}{\sqrt{6}}\left(\frac{1}{\sqrt{2}s_a}\underset{\sim}{s}^-_{\mu-1} - \frac{2}{\sqrt{2}s_b}\underset{\sim}{s}^-_{\mu} + \frac{1}{\sqrt{2}s_a}\underset{\sim}{s}^-_{\mu+1}\right)|\Omega\rangle, \\ |\Omega\rangle &= |m_0 = s_b, m_1 = s_a, \ldots, m_{N-1} = s_a\rangle, \end{aligned} \tag{2}$$

where μ is the position of the basal spin about which the localized magnon is centered, and $|\Omega\rangle$ denotes the magnon vacuum, i.e., the fully polarized state. These states are

*jschnack@uni-bielefeld.de

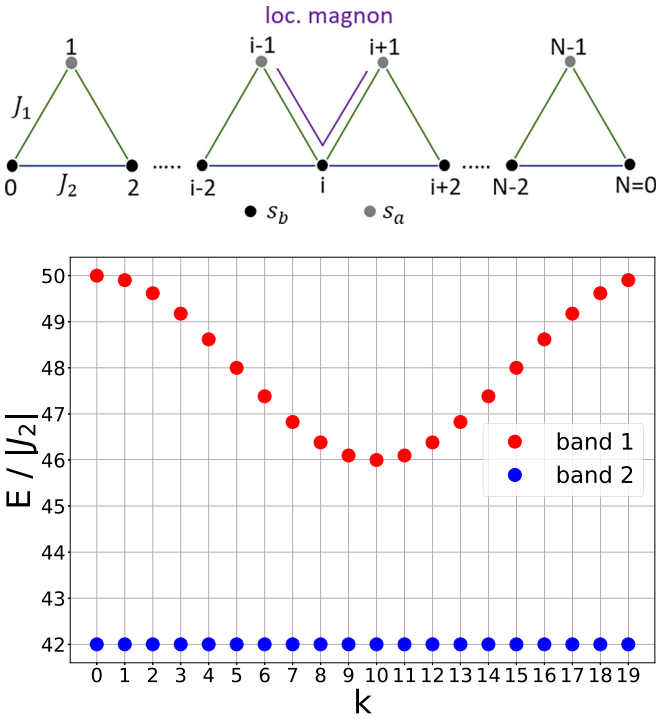

FIG. 1. Top: Structure of the delta chain with apical spins s_a and basal spins s_b as well as exchange interactions J_1 and J_2. The spins are numbered $0, 1, \ldots, N-1$. Periodic boundary conditions are applied, i.e., $N \equiv 0$. An independent localized one-magnon state is highlighted. It is a superposition of spin states with reduced magnetization [compare (2)] that extends over three neighboring sites as indicated. Bottom: Energy eigenvalues in one-magnon space for $N = 40$, $J_1 = -2$, $J_2 = -1$, and $s_a = s_b = \frac{1}{2}$. The momentum quantum number k (wave number) runs from 0 to $N/2 - 1$.

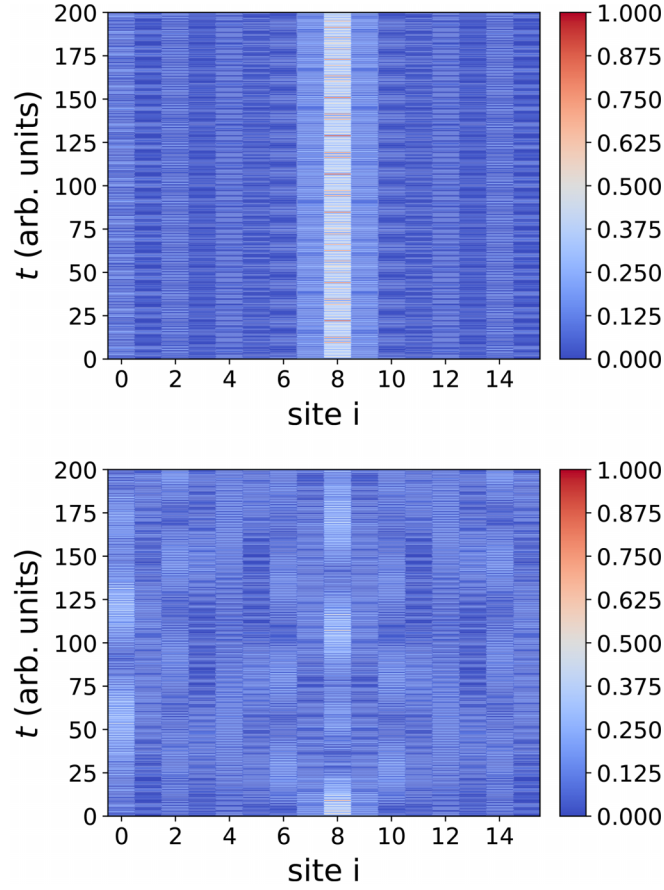

FIG. 2. $N = 16$, $s_a = s_b = s = 1/2$, $|\Psi(0)\rangle = \frac{1}{\sqrt{2s}} s_8^- |\Omega\rangle$: Magnetization dynamics for $\alpha = 0.5$ (top) as well as $\alpha = 0.48$ (bottom). The legend shows $0.5 - \langle s_i^z \rangle_t$.

eigenstates of Hamiltonian (1) with the same energy as the states of the flat band. Recently, localized independent one-magnon states have also been termed "compact localized states" [43,46,47], so often we will refer to them simply as localized states in this paper.

One expects that the dynamics is different in the case of a flat band compared to the generic case of dispersive bands. Qualitatively, the argument can be expressed in two ways: (1) Since one band is flat, the group velocity of these states is strictly zero, and therefore parts of a wave function belonging to the flat band will not move and therefore never equilibrate or thermalize. (2) Likewise, one can argue that the independent localized one-magnon states are stationary and contributions of them to a wave function stay localized where they started initially. Technically, the details are a bit more intricate since the localized one-magnon states are not mutually orthogonal; we will elaborate on this in Sec. III.

The following figures demonstrate the discussed dynamics by showing the local magnetization for all sites $i = 0, \ldots, N-1$, i.e.,

$$\langle s_i^z \rangle_t = \langle \Psi(t) | s_i^z | \Psi(t) \rangle, \tag{3}$$

$$|\Psi(0)\rangle = \frac{1}{\sqrt{2s_j}} s_j^- |\Omega\rangle, \tag{4}$$

starting with a single spin flip at site j at $t = 0$. We evaluated the dynamics both numerically as well as analytically, and the latter is shown [48,49].

We start our discussion by looking at single spin flips at a basal site j. One expects that these spin flips differ somewhat from flips at apical sites since they overlap only with one localized magnon whereas the latter overlap with two localized magnons (compare Fig. 1).

Figure 2 shows the magnetization dynamics for $N = 16$ and $s_a = s_b = s = \frac{1}{2}$ for the flat-band case $\alpha = J_2/J_1 = 1/2$ (top) as well as for a nearby Hamiltonian with $\alpha = 0.48$ (bottom), i.e., a dispersive band. As the initial state we choose $|\Psi(0)\rangle = \frac{1}{\sqrt{2s}} s_8^- |\Omega\rangle$. One can see that in the case of a flat band a large fraction of the magnetization remains localized at the position of the respective independent localized one-magnon state to which the site of the excitation belongs (sites 7–9 in the example) whereas for the (only slightly) dispersive band the magnetization delocalizes across the system. Since the system is rather small one observes to a small extent waves that run around the system due to periodic boundary conditions; they give rise to interferences.

The question is how larger systems behave. To this end we show results for $N = 40$ in Fig. 3 as well as $N = 200$ in Fig. 4. One clearly sees (top panel of both figures) that a

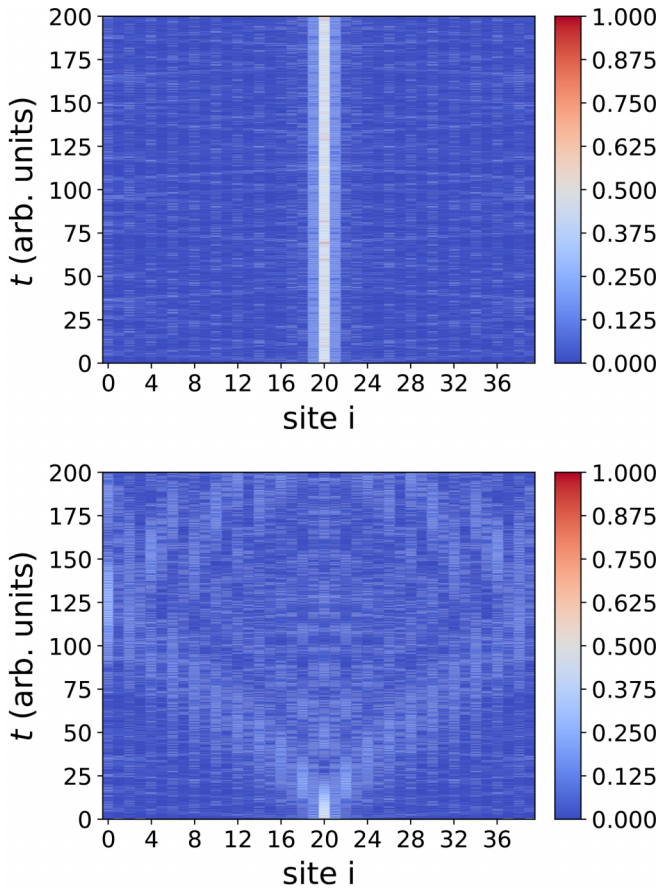

FIG. 3. $N = 40$, $s_a = s_b = s = 1/2$, $|\Psi(0)\rangle = \frac{1}{\sqrt{2s}} s^-_{\sim 20}|\Omega\rangle$: Magnetization dynamics for $\alpha = 0.5$ (top) as well as $\alpha = 0.48$ (bottom). The legend shows $0.5 - \langle s^z_{\sim i}\rangle_t$.

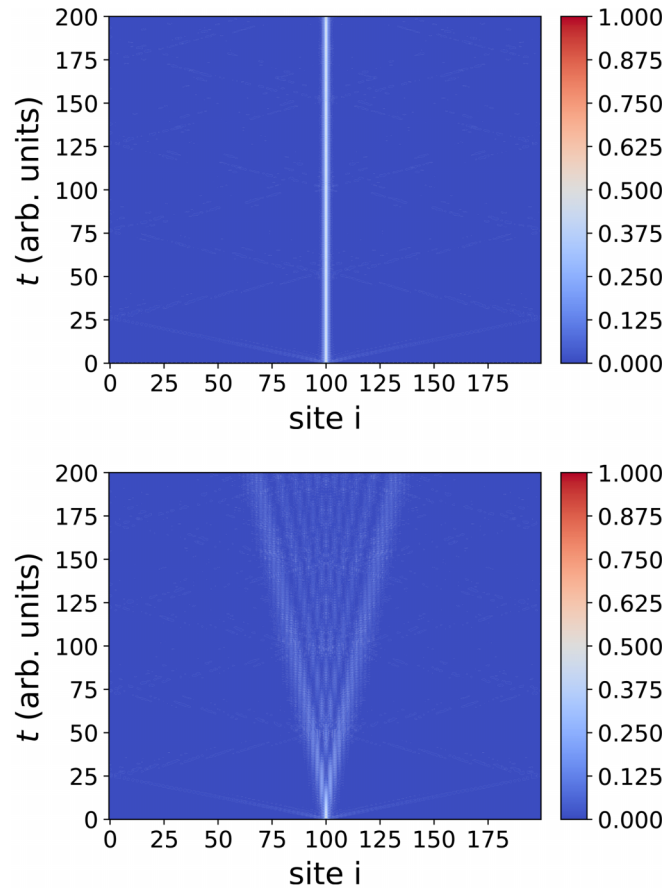

FIG. 4. $N = 200$, $s_a = s_b = s = 1/2$, $|\Psi(0)\rangle = \frac{1}{\sqrt{2s}} s^-_{\sim 100}|\Omega\rangle$: Magnetization dynamics for $\alpha = 0.5$ (top) as well as $\alpha = 0.48$ (bottom). The legend shows $0.5 - \langle s^z_{\sim i}\rangle_t$.

remanent magnetization persists at the site of the localized magnon overlapping with the single-spin excitation for the case of a flat band. In the case of dispersive bands the initially maximally localized magnetization fluctuation redistributes over the entire system (bottom panel of the figures).

The situation changes somewhat if the spin flip is executed at an apical site. Such a site belongs to two independent localized one-magnon states, therefore the magnetization remains dominantly localized across both states. It should also be somewhat smaller since it is now distributed over five sites.

Figures 5–7 display the cases of $N = 16$, $N = 40$, and $N = 200$, respectively. Again, the main insight we gain is that for the flat-band cases there is a remanent magnetization distributed about the site of the single spin flip whereas for the (only slightly) dispersive band the magnetization redistributes over the entire system.

We summarize our results graphically in Fig. 8 where we plot the time-averaged local magnetization, Eq. (3), at sufficiently late times for various sizes of the spin system, i.e.,

$$\overline{\langle s^z_{\sim i}\rangle}_t = \frac{1}{n_t \Delta t} \sum_{n=1}^{n_t} \langle \Psi(t + n\Delta t)|s^z_{\sim i}|\Psi(t + n\Delta t)\rangle. \quad (5)$$

We restrict ourselves to single-spin flips at a basal site. As one can see in Fig. 8 (top), the local magnetization at the site of the flip drops from one to 1/2 above background. At the neighboring sites that belong to the localized magnon $|\mu = j\rangle$ the local magnetization approaches roughly 0.1 above background. This means that out of the initial magnetization fluctuation about 70% remain localized at the respective localized magnon, a substantial fraction that never equilibrates. The precise contributions of a local spin flip that do not participate in an equilibrating dynamics will be exactly evaluated in Sec. III.

For the case of a dispersive band, shown in Fig. 8 (bottom), one immediately realizes that the magnetization fluctuation due to the single spin flip is practically evenly redistributed over the entire system. All late-time single-spin expectation values approach the background value of the magnon vacuum (set to zero) plus $1/N$ for the redistributed single spin flip.

Finally, since this is not the focus of the paper at hand, we refer readers interested in the question how exactly the system approaches its long-time limit to the existing extensive wealth of papers on that topic [26,28–32,50–53].

III. ANALYTICAL SOLUTION FOR THE DELTA CHAIN

All results discussed in Sec. II can be obtained either numerically or even analytically. An analytical solution for the delta chain can be achieved using the symmetries of

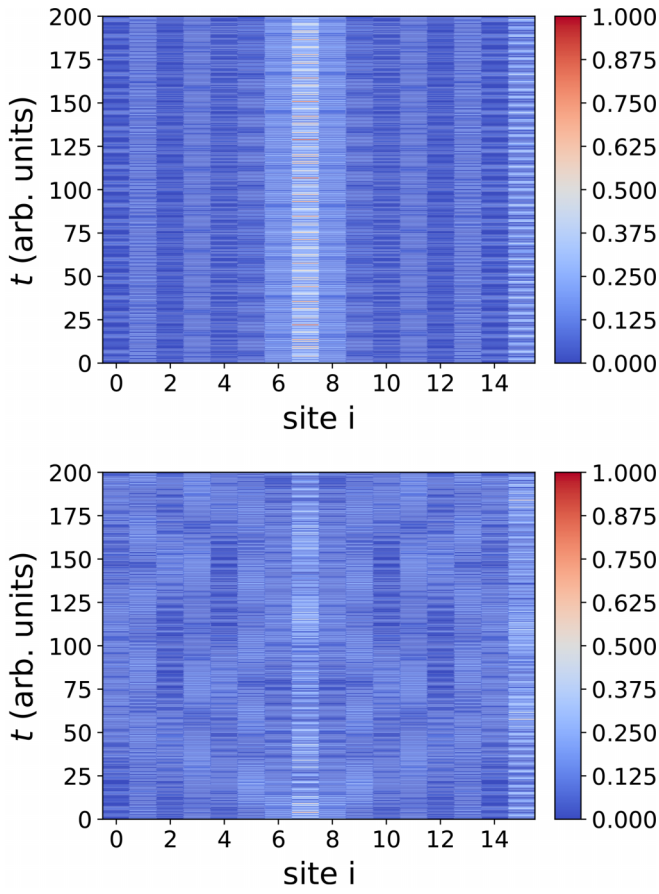

FIG. 5. $N = 16$, $s_a = s_b = 1/2$, $|\Psi(0)\rangle = \frac{1}{\sqrt{2}s_7}\underset{\sim}{s}_7^-|\Omega\rangle$: Magnetization dynamics for $\alpha = 0.5$ (top) as well as $\alpha = 0.48$ (bottom). The legend shows $0.5 - \langle \underset{\sim}{s}_i^z \rangle_t$.

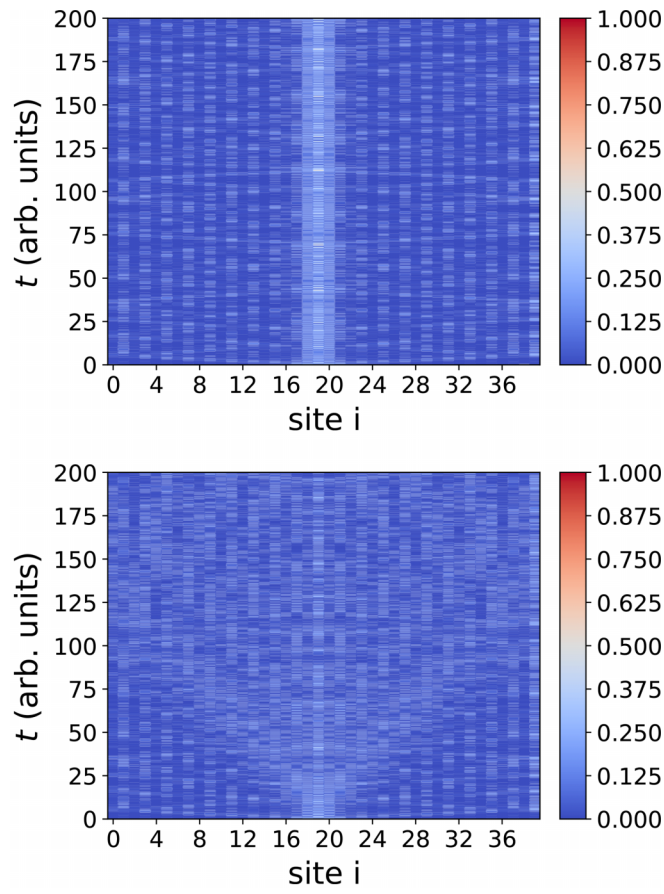

FIG. 6. $N = 40$, $s_a = s_b = s = 1/2$, $|\Psi(0)\rangle = \frac{1}{\sqrt{2}s}\underset{\sim}{s}_{19}^-|\Omega\rangle$: Magnetization dynamics for $\alpha = 0.5$ (top) as well as $\alpha = 0.48$ (bottom). The legend shows $0.5 - \langle \underset{\sim}{s}_i^z \rangle_t$.

the Hamiltonian. One-magnon space is spanned by N states $\frac{1}{\sqrt{2}s_i}\underset{\sim}{s}_i^-|\Omega\rangle$, and thus has got a dimension of N. A unit cell of the chain hosts two spins, one s_a and one s_b spin, respectively, with a translational symmetry given by the operator $\underset{\sim}{T}$, i.e.,

$$\underset{\sim}{T}|m_0, m_1, \ldots, m_{N-1}\rangle = |m_{N-2}, m_{N-1}, m_0, \ldots\rangle. \tag{6}$$

This leads to two bands of energy eigenvalues, each with $N/2$ states with momentum quantum numbers $k = 0, 1, \ldots, N/2 - 1$ [compare Fig. 1 (bottom)]. The energy eigenvalues $\epsilon_{k,\tau=\pm1}$ as well as eigenstates $|\epsilon_{k,\tau=\pm1}\rangle$ can be obtained analytically since the Hamiltonian matrix is only of size 2×2 for each value of k,

$$\begin{aligned}\epsilon_{k,1/2} = &-2J_1(Ns_as_b - s_a - s_b) - 2J_2\left\{\frac{N}{2}s_b^2 - s_b\right.\\ &\left.\times\left[1 - \cos\left(\frac{4\pi k}{N}\right)\right]\right\}\\ &\pm\left\{J_1^2 s_a^2 + 2J_1J_2s_as_b + (J_1 - J_2)^2\right.\\ &+ s_b\cos\left(\frac{4\pi k}{N}\right)\left[2(J_1 - J_2)(J_1s_a + J_2s_b)\right.\\ &\left.\left.+ J_2^2 s_b\cos\left(\frac{4\pi k}{N}\right)\right]\right\}^{1/2},\end{aligned} \tag{7}$$

where $\epsilon_{k,1}$ corresponds to the "+" sign and $\epsilon_{k,2}$ to the "−" sign, respectively. For $J_2 = J$ and $J_1 = 2J$ one obtains

$$\epsilon_{k,1} = -Js_b\left\{N(4s_a + s_b) - 4\left[1 - \cos\left(\frac{4\pi k}{N}\right)\right]\right\}, \tag{8}$$

$$\epsilon_{k,2} = -J\{4s_a(Ns_b - 2) + s_b(Ns_b - 8)\}, \tag{9}$$

where $\epsilon_{k,2}$ constitutes the flat band. The local magnetization at site j as displayed in Figs. 2–7 can analytically be evaluated as [48]

$$\begin{aligned}\langle\psi(t)|\underset{\sim}{s}_j^z|\psi(t)\rangle &= \langle\psi(0)|e^{\frac{i}{\hbar}\underset{\sim}{H}\cdot t}\underset{\sim}{s}_j^z e^{-\frac{i}{\hbar}\underset{\sim}{H}\cdot t}|\psi(0)\rangle\\ &= \sum_{k,\tau}\sum_{k',\tau'}\langle\psi(0)|\epsilon_{k,\tau}\rangle\langle\epsilon_{k,\tau}|\underset{\sim}{s}_j^z|\epsilon_{k',\tau'}\rangle\\ &\quad\times\langle\epsilon_{k',\tau'}|\psi(0)\rangle e^{\frac{i}{\hbar}(\epsilon_k^\tau - \epsilon_{k'}^{\tau'})\cdot t}.\end{aligned} \tag{10}$$

A deeper insight of the magnetization dynamics can be obtained by using a new basis in one-magnon space that consists of the localized magnons introduced in Eq. (2) and Fig. 1 complemented by analogous states constructed from the upper band,

$$|\phi_\mu^1\rangle = \frac{1}{\sqrt{6}}\left(\frac{1}{\sqrt{2s_b}}\underset{\sim}{s}_{\mu-1}^- + \frac{2}{\sqrt{2s_a}}\underset{\sim}{s}_\mu^- + \frac{1}{\sqrt{2s_b}}\underset{\sim}{s}_{\mu+1}^-\right)|\Omega\rangle. \tag{11}$$

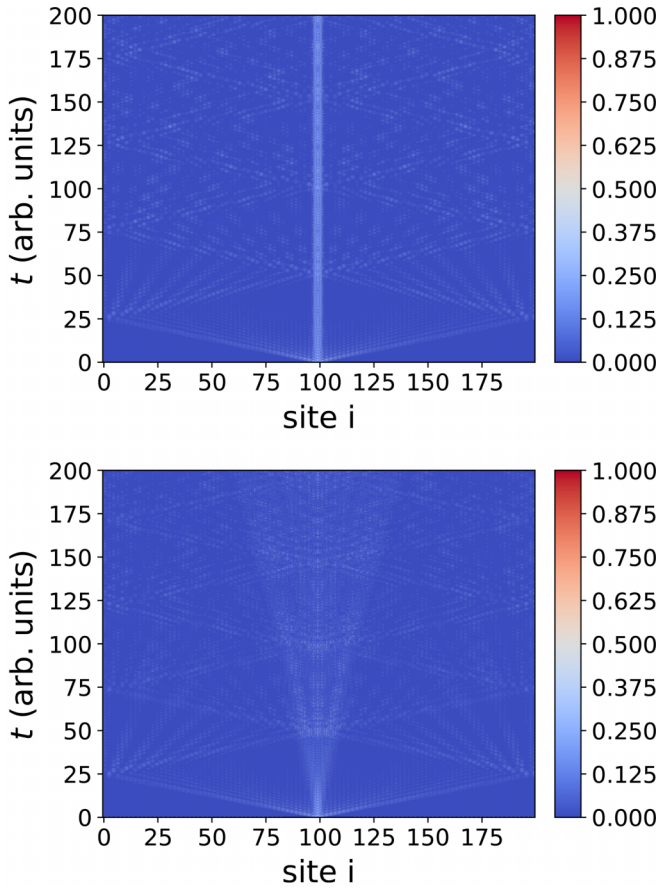

FIG. 7. $N = 200$, $s_a = s_b = s = 1/2$, $|\Psi(0)\rangle = \frac{1}{\sqrt{2}s} s^-_{99}|\Omega\rangle$: Magnetization dynamics for $\alpha = 0.5$ (top) as well as $\alpha = 0.48$ (bottom). The legend shows $0.5 - \langle s^z_i \rangle_t$.

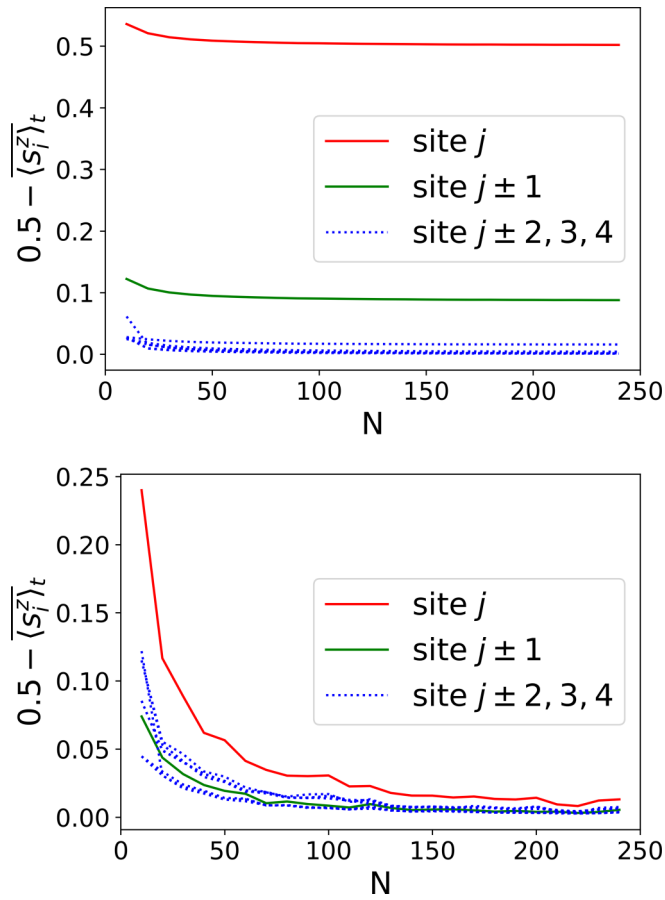

FIG. 8. Time-averaged local magnetization above background of magnon vacuum ($0.5 - \overline{\langle s^z_i \rangle_t}$) at sufficiently late times [compare (5)] for various sizes of the spin system: $\alpha = 0.5$ (top) and $\alpha = 0.48$ (bottom). All systems were time evolved over $t = 1\,000\,000$ of our time units and then averaged over an additional $n_t \Delta t = 2000$ time units [compare (5)].

We term the latter nonstationary localized magnon states; they are depicted in Fig. 9. For these states we find $\langle \phi^0_\mu | \phi^1_\nu \rangle = 0$, but otherwise they are not orthogonal. Although this complicates their use for easy (handwaving) interpretations of the results a little bit, the typical arguments we used in Sec. II resting, e.g., on overlaps are dominantly correct, i.e., up to small technical corrections.

A technically correct decomposition of the initial spin flip at site j,

$$\frac{1}{\sqrt{2}s_j} s^-_j |\Omega\rangle = \sum_{\mu=0,2,4,\ldots} c^{(j)}_\mu |\phi^0_\mu\rangle + \sum_{\mu=1,3,5,\ldots} c^{(j)}_\mu |\phi^1_\mu\rangle, \tag{12}$$

has to be performed, e.g., by a Householder QR decomposition. The coefficients $c^{(j)}_\mu$ are not given by dot products (overlaps) between the spin-flip state and the basis states as would be the case for an orthonormal basis. However, the easy (handwaving) interpretation used in Sec. II that the spin-flip state has got an overlap with a localized magnon (or two) and thus remains partially trapped at the site of the localized magnon remains true.

Figure 10 demonstrates for an example of a spin-flip state at a basal site how the coefficients $c^{(j)}_\mu$ fall off with growing distance $|\mu - j|$ from the site of the spin flip. The overwhelming weight is indeed taken by the localized magnon at that position, i.e., $\mu = j$. The two nearest localized magnons, $\mu = j \pm 2$, also carry some non-negligible, but already much smaller, weight. These contributions will also remain localized for all times. The numbers given in Fig. 10

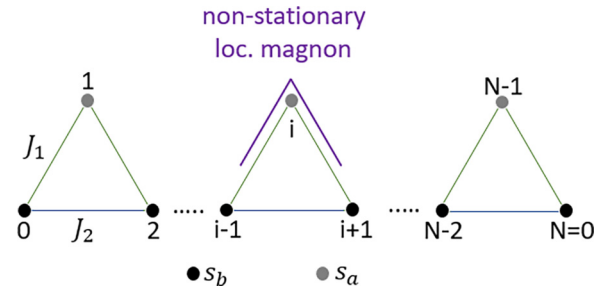

FIG. 9. Structure of the delta chain with apical spins s_a and basal spins s_b as well as exchange interactions J_1 and J_2. The spin are numbered $0, 1, \ldots, N-1$. Periodic boundary conditions are applied, i.e., $N \equiv 0$. A localized nonstationary one-magnon state is highlighted. It is a superposition of spin states with reduced magnetization [compare (11)] that extends over three neighboring sites as indicated.

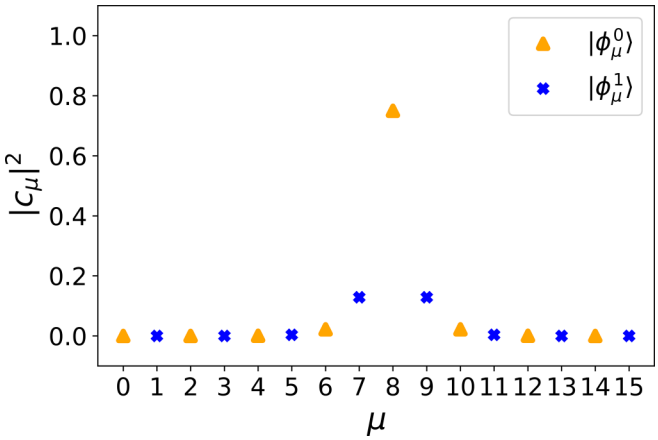

FIG. 10. Decomposition of a spin-flip state at a basal site into localized magnons and nonstationary localized magnons according to (12).

can be directly related to the long term averages given in Fig. 8.

The case of a spin-flip excitation at an apical side behaves very similarly and is therefore not shown. As anticipated, the contributions of the two localized magnons connected to that apical site is indeed largest, and contributions from localized magnons further away again fall off very rapidly.

IV. DISCUSSION AND CONCLUSIONS

In this paper, we demonstrated that certain carefully prepared Hamiltonians show nonergodic dynamics in contrast to the vast number of generic Hamiltonians nearby in some parameter space. In our demonstration, the behavior can be traced back to the influence of a perfectly flat energy band that is characterized by zero group velocity or equivalently by independent localized one-magnon states that are eigenstates of the Hamiltonian and therefore stationary. The latter phenomenon has thus been termed "disorder-free localization." It is an interference effect due to the fine-tuned frustration of the competing interactions J_1 and J_2 [54].

One important aspect of our investigation is that we can evaluate all quantities analytically [48], and thus do not rely on numerics. In addition, our use of nonorthogonal basis states is technically involved, but offers the prospect of a better understanding of the phenomenon [55–59]. In particular, it allows us to understand which stationary localized one-magnon states contribute to a certain initial state, e.g., a single spin flip.

Although we only investigated the time evolution of single spin flips on the background of a magnon vacuum the results can be easily transferred to arbitrary initial states in one-magnon space since these can be written as superpositions of single spin-flip states. Furtheron, our investigations hold for general spin quantum numbers; the respective formulas are expressed in terms of s_a and s_b.

Flat bands appear for all kinds of Hamiltonians and have initially been investigated for the Hubbard model [33]. It is therefore no surprise that observations similar to ours have been discussed in connection with Hubbard models [60,61]. Many flat-band systems have a realization as a magnetic material, for instance, kagome or pyrochlore systems. Recently, the idea was brought up that Hamiltonians of such systems can be tuned by electric fields in order to set up a flat-band scenario [45]. This can potentially be achieved with multiferroic materials as, e.g., discussed in Ref. [62].

In an antiferromagnetic delta chain, one-magnon states are highly excited states close to the upper end of the spectrum. They can be turned into low-lying states by means of a magnetic field. However, for real materials such a field close to the saturation field might not be small and thus experimentally hard to achieve. Some years ago, a new class of models with mixed ferromagnetic-antiferromagnetic interaction patterns had been invented that exhibit similar properties at zero field [63]. For the discussed delta chain chemical compounds could be synthesized that resemble these properties rather closely [64,65]. In addition, a second class of spin models featuring flat bands was suggested. These models are defined by special XXZ couplings [66,67]. This large variety demonstrates that among the generic Hamiltonians interesting fine-tuned Hamiltonians exist that show exciting frustration properties [68], among which nongeneric long-time behavior is an interesting aspect.

ACKNOWLEDGMENTS

We thank M. Haque and J. Richter for discussions. This work was supported by the Deutsche Forschungsgemeinschaft DFG [355031190 (FOR 2692); 397300368 (SCHN 615/25-2)].

[1] J. M. Deutsch, Quantum statistical mechanics in a closed system, Phys. Rev. A **43**, 2046 (1991).
[2] M. Srednicki, Chaos and quantum thermalization, Phys. Rev. E **50**, 888 (1994).
[3] J. Schnack and H. Feldmeier, Statistical properties of fermionic molecular dynamics, Nucl. Phys. A **601**, 181 (1996).
[4] H. Tasaki, From Quantum Dynamics to the Canonical Distribution: General Picture and a Rigorous Example, Phys. Rev. Lett. **80**, 1373 (1998).
[5] M. Rigol, V. Dunjko, and M. Olshanii, Thermalization and its mechanism for generic isolated quantum systems, Nature (London) **452**, 854 (2008).
[6] A. Polkovnikov, K. Sengupta, A. Silva, and M. Vengalattore, Colloquium: Nonequilibrium dynamics of closed interacting quantum systems, Rev. Mod. Phys. **83**, 863 (2011).
[7] P. Reimann and M. Kastner, Equilibration of isolated macroscopic quantum systems, New J. Phys. **14**, 043020 (2012).
[8] R. Steinigeweg, A. Khodja, H. Niemeyer, C. Gogolin, and J. Gemmer, Pushing the Limits of the Eigenstate Thermalization Hypothesis towards Mesoscopic Quantum Systems, Phys. Rev. Lett. **112**, 130403 (2014).
[9] C. Gogolin and J. Eisert, Equilibration, thermalisation, and the emergence of statistical mechanics in closed quantum systems, Rep. Prog. Phys. **79**, 056001 (2016).

[10] L. D'Alessio, Y. Kafri, A. Polkovnikov, and M. Rigol, From quantum chaos and eigenstate thermalization to statistical mechanics and thermodynamics, Adv. Phys. **65**, 239 (2016).

[11] F. Borgonovi, F. M. Izrailev, L. F. Santos, and V. G. Zelevinsky, Quantum chaos and thermalization in isolated systems of interacting particles, Phys. Rep. **626**, 1 (2016).

[12] Y.-L. Wu, D.-L. Deng, X. Li, and S. Das Sarma, Intrinsic decoherence in isolated quantum systems, Phys. Rev. B **95**, 014202 (2017).

[13] In the context of this paper, equilibration denotes a long-term behavior in which expectation values become stationary for the vast majority of late times and assume the same value for symmetry-equivalent operators.

[14] C. J. Turner, A. A. Michailidis, D. A. Abanin, M. Serbyn, and Z. Papić, Weak ergodicity breaking from quantum many-body scars, Nat. Phys. **14**, 745 (2018).

[15] C. J. Turner, A. A. Michailidis, D. A. Abanin, M. Serbyn, and Z. Papić, Quantum scarred eigenstates in a Rydberg atom chain: Entanglement, breakdown of thermalization, and stability to perturbations, Phys. Rev. B **98**, 155134 (2018).

[16] W. W. Ho, S. Choi, H. Pichler, and M. D. Lukin, Periodic Orbits, Entanglement, and Quantum Many-Body Scars in Constrained Models: Matrix Product State Approach, Phys. Rev. Lett. **122**, 040603 (2019).

[17] P. A. McClarty, M. Haque, A. Sen, and J. Richter, Disorder-free localization and many-body quantum scars from magnetic frustration, Phys. Rev. B **102**, 224303 (2020).

[18] Y. Kuno, T. Mizoguchi, and Y. Hatsugai, Flat band quantum scar, Phys. Rev. B **102**, 241115(R) (2020).

[19] S. Pilatowsky-Cameo, D. Villaseñor, M. A. Bastarrachea-Magnani, S. Lerma-Hernández, L. F. Santos, and J. G. Hirsch, Ubiquitous quantum scarring does not prevent ergodicity, Nat. Commun. **12**, 852 (2021).

[20] S. A. Crooker, D. D. Awschalom, J. J. Baumberg, F. Flack, and N. Samarth, Optical spin resonance and transverse spin relaxation in magnetic semiconductor quantum wells, Phys. Rev. B **56**, 7574 (1997).

[21] N. Mizuochi, P. Neumann, F. Rempp, J. Beck, V. Jacques, P. Siyushev, K. Nakamura, D. J. Twitchen, H. Watanabe, S. Yamasaki, F. Jelezko, and J. Wrachtrup, Coherence of single spins coupled to a nuclear spin bath of varying density, Phys. Rev. B **80**, 041201(R) (2009).

[22] Ł. Cywiński, W. M. Witzel, and S. Das Sarma, Electron Spin Dephasing due to Hyperfine Interactions with a Nuclear Spin Bath, Phys. Rev. Lett. **102**, 057601 (2009).

[23] A. Ardavan, O. Rival, J. J. L. Morton, S. J. Blundell, A. M. Tyryshkin, G. A. Timco, and R. E. P. Winpenny, Will Spin-Relaxation Times in Molecular Magnets Permit Quantum Information Processing? Phys. Rev. Lett. **98**, 057201 (2007).

[24] P. N. Jepsen, W. W. Ho, J. Amato-Grill, I. Dimitrova, E. Demler, and W. Ketterle, Transverse Spin Dynamics in the Anisotropic Heisenberg Model Realized with Ultracold Atoms, Phys. Rev. X **11**, 041054 (2021).

[25] P. Vorndamme, H.-J. Schmidt, C. Schröder, and J. Schnack, Observation of phase synchronization and alignment during free induction decay of quantum spins with Heisenberg interactions, New J. Phys. **23**, 083038 (2021).

[26] R. Steinigeweg, J. Herbrych, and P. Prelovšek, Eigenstate thermalization within isolated spin-chain systems, Phys. Rev. E **87**, 012118 (2013).

[27] B. N. Balz and P. Reimann, Typical Relaxation of Isolated Many-Body Systems Which Do Not Thermalize, Phys. Rev. Lett. **118**, 190601 (2017).

[28] R. Steinigeweg, F. Jin, D. Schmidtke, H. De Raedt, K. Michielsen, and J. Gemmer, Real-time broadening of nonequilibrium density profiles and the role of the specific initial-state realization, Phys. Rev. B **95**, 035155 (2017).

[29] R. Steinigeweg, F. Jin, H. De Raedt, K. Michielsen, and J. Gemmer, Charge diffusion in the one-dimensional Hubbard model, Phys. Rev. E **96**, 020105(R) (2017).

[30] J. Richter, F. Jin, H. De Raedt, K. Michielsen, J. Gemmer, and R. Steinigeweg, Real-time dynamics of typical and untypical states in nonintegrable systems, Phys. Rev. B **97**, 174430 (2018).

[31] J. Richter, F. Jin, L. Knipschild, J. Herbrych, H. De Raedt, K. Michielsen, J. Gemmer, and R. Steinigeweg, Magnetization and energy dynamics in spin ladders: Evidence of diffusion in time, frequency, position, and momentum, Phys. Rev. B **99**, 144422 (2019).

[32] B. Bertini, F. Heidrich-Meisner, C. Karrasch, T. Prosen, R. Steinigeweg, and M. Žnidarič, Finite-temperature transport in one-dimensional quantum lattice models, Rev. Mod. Phys. **93**, 025003 (2021).

[33] A. Mielke and H. Tasaki, Ferromagnetism in the Hubbard-model – examples from models with degenerate single-electron ground-states, Commun. Math. Phys. **158**, 341 (1993).

[34] J. Schnack, H.-J. Schmidt, J. Richter, and J. Schulenburg, Independent magnon states on magnetic polytopes, Eur. Phys. J. B **24**, 475 (2001).

[35] J. Schulenburg, A. Honecker, J. Schnack, J. Richter, and H.-J. Schmidt, Macroscopic Magnetization Jumps due to Independent Magnons in Frustrated Quantum Spin Lattices, Phys. Rev. Lett. **88**, 167207 (2002).

[36] S. A. Blundell and M. D. Núñez-Regueiro, Quantum topological excitations: from the sawtooth lattice to the Heisenberg chain, Eur. Phys. J. B **31**, 453 (2003).

[37] J. Richter, J. Schulenburg, A. Honecker, J. Schnack, and H.-J. Schmidt, Exact eigenstates and macroscopic magnetization jumps in strongly frustrated spin lattices, J. Phys.: Condens. Matter **16**, S779 (2004).

[38] H.-J. Schmidt, J. Richter, and R. Moessner, Linear independence of localized magnon states, J. Phys. A: Math. Gen. **39**, 10673 (2006).

[39] M. E. Zhitomirsky and H. Tsunetsugu, Exact low-temperature behavior of a kagomé antiferromagnet at high fields, Phys. Rev. B **70**, 100403(R) (2004).

[40] O. Derzhko, J. Richter, A. Honecker, M. Maksymenko, and R. Moessner, Low-temperature properties of the Hubbard model on highly frustrated one-dimensional lattices, Phys. Rev. B **81**, 014421 (2010).

[41] M. Maksymenko, A. Honecker, R. Moessner, J. Richter, and O. Derzhko, Flat-Band Ferromagnetism as a Pauli-Correlated Percolation Problem, Phys. Rev. Lett. **109**, 096404 (2012).

[42] A. Mielke, Exact ground states for the Hubbard model on the Kagome lattice, J. Phys. A: Math. Gen. **25**, 4335 (1992).

[43] D. Leykam, A. Andreanov, and S. Flach, Artificial flat band systems: from lattice models to experiments, Adv. Phys.: X **3**, 1473052 (2018).

[44] S. Tilleke, M. Daumann, and T. Dahm, Nearest neighbour particle-particle interaction in fermionic quasi one-dimensional flat band lattices, Z. Naturforsch. A **75**, 393 (2020).

[45] J. Richter, V. Ohanyan, J. Schulenburg, and J. Schnack, Electric field driven flat bands: Enhanced magnetoelectric and electrocaloric effects in frustrated quantum magnets, Phys. Rev. B **105**, 054420 (2022).

[46] W. Maimaiti, A. Andreanov, H. C. Park, O. Gendelman, and S. Flach, Compact localized states and flat-band generators in one dimension, Phys. Rev. B **95**, 115135 (2017).

[47] Y. Chen, J. Huang, K. Jiang, and J. Hu, Decoding flat bands from compact localized states, arXiv:2212.13526.

[48] F. Johannesmann, Dynamik im Einmagnonenraum der Heisenberg-Delta-Kette, Bachelor thesis, Bielefeld University, 2022.

[49] J. Eckseler, Lokale Remanenz und globale Synchronisation unter unitärer Zeitentwicklung in Quantenspinsystemen am Beispiel zweier Heisenberg-Systeme, Master thesis, Bielefeld University, 2023.

[50] F. Heidrich-Meisner, A. Honecker, D. C. Cabra, and W. Brenig, Thermal conductivity of anisotropic and frustrated spin-$\frac{1}{2}$ chains, Phys. Rev. B **66**, 140406(R) (2002).

[51] F. Heidrich-Meisner, A. Honecker, D. C. Cabra, and W. Brenig, Zero-frequency transport properties of one-dimensional spin-$\frac{1}{2}$ systems, Phys. Rev. B **68**, 134436 (2003).

[52] C. Karrasch, J. E. Moore, and F. Heidrich-Meisner, Real-time and real-space spin and energy dynamics in one-dimensional spin-$\frac{1}{2}$ systems induced by local quantum quenches at finite temperatures, Phys. Rev. B **89**, 075139 (2014).

[53] C. B. Krimphoff, M. Haque, and A. M. Läuchli, Propagation and jamming dynamics in Heisenberg spin ladders, Phys. Rev. B **95**, 144308 (2017).

[54] O. Derzhko, J. Richter, and M. Maksymenko, Strongly correlated flat-band systems: The route from Heisenberg spins to Hubbard electrons, Int. J. Mod. Phys. B **29**, 1530007 (2015).

[55] H. Tasaki, Ferromagnetism in the Hubbard Models with Degenerate Single-Electron Ground States, Phys. Rev. Lett. **69**, 1608 (1992).

[56] H. Tasaki, From Nagaoka's ferromagnetism to flat-band ferromagnetism and beyond – an introduction to ferromagnetism in the Hubbard model, Prog. Theor. Phys. **99**, 489 (1998).

[57] T. Mizoguchi and Y. Hatsugai, Molecular-orbital representation of generic flat-band models, Europhys. Lett. **127**, 47001 (2019).

[58] A. Tanaka, An extension of the cell-construction method for the flat-band ferromagnetism, J. Stat. Phys. **181**, 897 (2020).

[59] H. Katsura, N. Kawashima, S. Morita, A. Tanaka, and H. Tasaki, Mott-insulator-like Bose-Einstein condensation in a tight-binding system of interacting bosons with a flat band, Phys. Rev. Res. **3**, 033190 (2021).

[60] M. Daumann, R. Steinigeweg, and T. Dahm, Many-body localization in translational invariant diamond ladders with flat bands, Phys. Rev. B **108**, 045129 (2023).

[61] M. Daumann, Violation of eigenstate thermalization and anomalous diffusion in flat band systems, Ph.D. thesis, Bielefeld University, 2022.

[62] H. C. Mandujano, A. Metta, N. Barišić, Q. Zhang, W. Tabiś, N. K. C. Muniraju, and H. S. Nair, Sawtooth lattice multiferroic $BeCr_2O_4$: Noncollinear magnetic structure and multiple magnetic transitions, Phys. Rev. Mater. **7**, 024422 (2023).

[63] V. Y. Krivnov, D. V. Dmitriev, S. Nishimoto, S.-L. Drechsler, and J. Richter, Delta chain with ferromagnetic and antiferromagnetic interactions at the critical point, Phys. Rev. B **90**, 014441 (2014).

[64] Y. Inagaki, Y. Narumi, K. Kindo, H. Kikuchi, T. Kamikawa, T. Kunimoto, S. Okubo, H. Ohta, T. Saito, M. Azuma, M. Takano, H. Nojiri, M. Kaburagi, and T. Tonegawa, Ferro-antiferromagnetic delta-chain system studied by high field magnetization measurements, J. Phys. Soc. Jpn. **74**, 2831 (2005).

[65] A. Baniodeh, N. Magnani, Y. Lan, G. Buth, C. E. Anson, J. Richter, M. Affronte, J. Schnack, and A. K. Powell, High spin cycles: topping the spin record for a single molecule verging on quantum criticality, npj Quantum Mater. **3**, 10 (2018).

[66] H. J. Changlani, D. Kochkov, K. Kumar, B. K. Clark, and E. Fradkin, Macroscopically Degenerate Exactly Solvable Point in the Spin-1/2 Kagome Quantum Antiferromagnet, Phys. Rev. Lett. **120**, 117202 (2018).

[67] H. J. Changlani, S. Pujari, C.-M. Chung, and B. K. Clark, Resonating quantum three-coloring wave functions for the kagome quantum antiferromagnet, Phys. Rev. B **99**, 104433 (2019).

[68] J. Schnack, Large magnetic molecules and what we learn from them, Contemp. Phys. **60**, 127 (2019).